DALTON
FULL PAPER

Exchange-coupled high-spin, low-spin and spin-crossover dicobalt(II) complexes of a pyridazine-containing Schiff-base macrocycle: control of cobalt(II) spin state by choice of axial ligands

Sally Brooker,*[a] Duncan J. de Geest,[a] Robert J. Kelly,[a] Paul G. Plieger,[a] Boujemaa Moubaraki,[b] Keith S. Murray*[b] and Geoffrey B. Jameson[c]

[a] *Department of Chemistry, University of Otago, PO Box 56, Dunedin, New Zealand. E-mail: sbrooker@alkali.otago.ac.nz*
[b] *School of Chemistry, Monash University, PO Box 23, Clayton, Victoria 3800, Australia*
[c] *Institute of Fundamental Sciences, Chemistry, Massey University, PO Box 11222, Palmerston North, New Zealand*

Received 11th December 2001, Accepted 19th February 2002
First published as an Advance Article on the web 2nd April 2002

A series of doubly pyridazine-bridged dicobalt(II) macrocyclic complexes, **1**–**7**, is reported. The pyridazine-containing Schiff-base macrocycle L1 [derived from the (2 + 2) condensation of 3,6-diformylpyridazine and 1,3-diaminopropane] provides four nitrogen donor atoms, disposed in an approximately square-planar manner, to each cobalt ion. Variation of the axial donors alters the spin state of the cobalt(II) ions from high spin, $[Co_2L1(H_2O)_4](ClO_4)_4$ (**2**), $[Co_2L1(H_2O)_4](S_2O_6)_2\cdot 4(H_2O)$ (**3**·8H_2O), $[Co_2L1(N_3)_2](ClO_4)_2$ (**4**) and $[Co_2L1(NCO)_3]ClO_4$ (**5**), to spin crossover, $[Co_2L1(MeCN)_4](ClO_4)_4$ (**1**·4MeCN) and $[Co_2L1(NCS)_2(SCN)_2]$ (**6**), to low spin, $[Co_2L1Cl_2](ClO_4)_2$ (**7**). Detailed magnetic susceptibility studies have yielded small, negative 2*J* values (−7 to −20 cm^{-1}) for complexes **2** to **5**. Compounds **1**, **1**·4MeCN and **6** are rare examples of binuclear complexes displaying simultaneous spin crossover (3/2 ⇔ 1/2) at high temperatures and antiferromagnetic exchange of the low-spin d^7–d^7 ions at low temperatures ($2J = -10$ to -14 cm^{-1}).

Introduction

We have recently added 3,6-diformylpyridazine to the range of dicarbonyl "head units" used in Schiff-base macrocyclic chemistry[1–8] and, as a consequence, dicopper and dicobalt complexes with unusual electrochemical properties have been reported.[3,4,6,7] The pyridazine moieties doubly bridge the metal ions in these macrocyclic complexes[1–8] and are well known to mediate magnetic exchange,[9] so the complexes also possess interesting magnetic properties.[3,5,7] Specifically, we are interested in the preparation and full characterisation of single molecules and arrays of molecules which might ultimately act as nanoswitches or memory devices. A reversible spin transition, low ⇔ high spin, as the temperature, pressure or visible light irradiation is varied causes a change in colour and magnetism and is an example of bistability, which is required for a nanoswitch. Taking this a step further, a memory device based on magnetic properties would require a spin transition with hysteresis.[10–12]

The vast majority of examples of spin-transition complexes are of iron,[13] but numerous examples involving cobalt are also known.[14] Here, we report the cobalt coordination chemistry of the pyridazine-containing Schiff-base macrocycle L1 (Fig. 1). Prior to this work, no other macrocyclic pyridazine-bridged cobalt(II) complexes, with the exception of one phthalazine-containing example,[15] and only a handful of cobalt complexes of pyridazine-containing acyclic ligands,[16–19] had been reported and, in all cases, the pyridazine-bridged cobalt ions were high-spin. In contrast, the macrocycle L1 has allowed us to isolate and characterise a series of dicobalt(II) complexes with a range of spin states. The complex $[Co_2L1(MeCN)_4](ClO_4)_4$ (**1**·4MeCN), in addition to exhibiting interesting redox chemistry, has been shown to be a rare example of a cobalt(II) complex which undergoes a gradual, incomplete, spin transition,[4] as does the thiocyanate derivative $[Co_2L1(NCS)_2(SCN)_2]$ (**6**).[5] In an effort to expand the range of spin states and to form arrays of these complexes, derivatives of complex **1** have been prepared and we report here the synthesis, structures and characterisation of this series of dicobalt(II) complexes. Comparisons are made with recently reported Fe^{II}(μ-bipyrimidine)Fe^{II} systems by Real *et al.*[20]

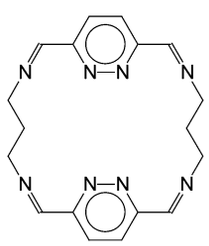

Fig. 1 Pyridazine-containing Schiff-base macrocycle L1.

Results and discussion

Synthesis and characterisation

The complex $[Co_2L1](ClO_4)_4$ (**1**) is prepared in good yield by transmetallation of $[Pb_2(4 + 4)](ClO_4)_4$ with four equivalents of $Co(ClO_4)_2\cdot 6H_2O$.[4] Ring contraction of the (4 + 4) macrocycle to the (2 + 2) macrocycle occurs, as it has in all other transmetallations to date.[2–7] Direct reaction of the macrocycle components, 3,6-diformylpyridazine and 1,3-diaminopropane, using cobalt(II) as a template ion failed to produce **1**.

The addition of a small quantity of water (~9% by volume) to an acetonitrile solution of **1** changed the colour from deep red to bright orange. Slow diffusion of diethyl ether into this orange solution gave the complex $[Co_2L1(H_2O)_4](ClO_4)_4$ (**2**) as orange rods of **2**·2H_2O·2MeCN. Reactions of **1** in water with

 DOI: 10.1039/b111267h

appropriate anions gave $[Co_2L1](S_2O_6)_2$ (**3**) and $[Co_2L1(N_3)_2](ClO_4)_2$ (**4**). The orange dithionate complex is initially isolated as the aquo adduct (*vide infra*), but is dried *in vacuo* to give **3**. Addition of two equivalents of NaN_3 to **1** resulted in the isolation of the orange–brown diazide complex **4**. Similarly, reactions of the deep red tetraacetonitrile adduct of **1**, $[Co_2L1(MeCN)_4](ClO_4)_4$, in MeCN with appropriate anions led to the formation of the complexes $[Co_2L1(NCO)_3]ClO_4$ (**5**), $[Co_2L1(NCS)_2(SCN)_2]$ (**6**) and $[Co_2L1Cl_2](ClO_4)_2$ (**7**). In the case of the orange cyanate complex **5**, the addition of two equivalents of NaOCN resulted in the crystallisation of the desired product, along with unreacted **1**. Four equivalents of NaOCN gave **5** contaminated with excess NaOCN. As there was no evidence for the formation of either di- or tetracyanate complexes, three equivalents of NaOCN were used to give clean tricyanate product. In the case of the black tetrathiocyanate complex **6**, a large excess of NaNCS was needed to ensure complete reaction, although some of the tetrathiocyanate complex was formed even when only two equivalents of NCS^- were present. The intense purple–black dichloride complex **7** was formed from **1** by adding a stoichiometric amount of $Et_4NCl{\cdot}H_2O$.

Attempts to further exploit the unique ligand field balance provided to cobalt(II) by the macrocyclic ligand L1 have been made. Specifically, efforts have focussed on coordinating a variety of bridging groups which may mediate magnetic exchange between the $[Co_2L1]^{4+}$ units, as it is recognised that this could facilitate the formation of the extended arrays required for a more abrupt transition and hysteresis effects. The ladder array formed in the case of the closely related dicopper(II) complex, $\{[Cu_2L1Cl_2]^{2+}\}_x$, provides a structural precedent for the desired cobalt(II) arrays.[7] However, despite employing a wide range of ligands, including nitrile derivatives (*e.g.* 4-cyanopyridine, dicyanamide, cyanamide), pyridines [*e.g.* 4,4′-bipyridine, 4-aminopyridine, 4-(aminomethyl)pyridine, *trans*-1,2-bis(4-pyridyl)ethylene], "simple" anions (*e.g.* bromide, iodide, hydroxide, acetate), complex anions (*e.g.* ferricyanide, ferrocyanide), *para*-dihydroxybenzene and *para*-dicarboxybenzene, in a wide range of both non-coordinating and coordinating solvents (solvent choice was limited by solubility considerations but, where possible, included acetonitrile, nitromethane, acetone, water and methanol), no clean products have been obtained from these experiments to date. Indeed, in the cases of cyanamide and 4-cyanopyridine, the starting materials were reclaimed.

As expected, the IR spectra of the complexes **1**–**7** have many similar features. Characteristic stretches due to aromatic C–H (*ca.* 3060 cm^{-1}), alkyl C–H (2854–2949 cm^{-1}), imine C=N (*ca.* 1652 cm^{-1}) and pyridazine ring C–C and C–N (*ca.* 1584 and 1554 cm^{-1}) bonds are present in all the spectra. The sharp perchlorate bands (*ca.* 1085 and 625 cm^{-1}) observed for the complexes **2**, **4**, **5** and **7** show no signs of peak splitting, so the perchlorate ions are not expected to show any significant interactions with the respective complexes. The infrared spectrum of $[Co_2L1](S_2O_6)_2$ (**3**) is dominated by the two strong absorptions due to the anion at 1245 and 991 cm^{-1}.[21] In the anhydrous solid, these peaks show no evidence of splitting, indicating that, in the absence of the hydrogen bonds observed in the solid state structure of the hydrated material, there is no interaction between these anions and the complex cation. In the case of $[Co_2L1(NCS)_2(SCN)_2]$ (**6**), there is only one, slightly asymmetric, thiocyanate stretch (2074 cm^{-1}). The solid state structure of **6** (*vide infra*)[5] clearly shows two different binding modes for the coordinated thiocyanate ions, with both N-bound and S-bound monodentate thiocyanate ions present, but, the typical ranges for these binding modes overlap.[22] The complex $[Co_2L1(N_3)_2](ClO_4)_2$ (**4**) exhibits one band at 2033 cm^{-1}, which is more typical of an end-on coordinated azide ion than either a 1,1 or 1,3 bridge, but is not definitive.[22] The infrared spectrum of the cyanate complex $[Co_2L1(NCO)_3]ClO_4$ (**5**) shows two closely positioned bands at 2196 and 2155 cm^{-1}, which are attributed to the bridging and terminal modes of the coordinated cyanate ions, respectively.[23]

Conductivity measurements were performed on all compounds that showed sufficient solubility to achieve 1 mmol L^{-1} concentration in acetonitrile, DMF or water: this precluded a study on $[Co_2L1(NCS)_2(SCN)_2]$ (**6**). Complex **1** in acetonitrile solution is a 3 : 1 conductor. The molar conductivity of an orange aqueous solution of $[Co_2L1(H_2O)_4](ClO_4)_4$ (**2**) is just above the literature value for a 3 : 1 electrolyte, whereas that of an orange aqueous solution of $[Co_2L1](S_2O_6)_2$ (**3**) is just above the literature value for a 2 : 1 electrolyte. The discrepancies are probably due to mobility effects.[24] The molar conductivity of an orange aqueous solution (not sufficiently soluble in MeCN) of $[Co_2L1(N_3)_2](ClO_4)_2$ (**4**) is just within the literature range for a 3 : 1 electrolyte. Given the preference this complex shows for two equivalents of azide ion, it is expected that both azide anions are bound in the solid state (the infrared spectrum of the isolated complex shows only one band), so this result implies that, in aqueous solution, one of these azide anions is displaced. An orange acetonitrile solution of $[Co_2L1(NCO)_3]ClO_4$ (**5**) has a molar conductivity in the literature range for a 1 : 1 electrolyte. The deep purple–black complex $[Co_2L1Cl_2](ClO_4)_2$ (**7**) eventually dissolves in DMF to give an orange solution, with a molar conductivity value slightly lower than the literature value for a 2 : 1 electrolyte, and this is probably due to a change in coordination environment and spin state around cobalt.

UV-visible spectra were recorded for those complexes which had sufficient solubility in acetonitrile, DMF or water: this precluded a study on **6**. All of the other complexes showed an intense absorbance from 354–407 nm due to a charge-transfer transition. In addition, the octahedral high-spin complex $[Co_2L1(NCO)_3]ClO_4$ (**5**) has a d–d transition at 918 nm (ε = 11 $dm^3\ mol^{-1}\ cm^{-1}$) and the octahedral high-spin complex $[Co_2L1(H_2O)_4](ClO_4)_4$ (**2**) has two d–d transitions at 841 (9) and 965 nm (6 $dm^3\ mol^{-1}\ cm^{-1}$). Similarly, the spectrum of an aqueous solution of the analogous complex $[Co_2L1](S_2O_6)_2$ (**3**), which would be expected to bind water axially as well and thus form an identical complex cation, has a d–d transition at 839 nm (18 $dm^3\ mol^{-1}\ cm^{-1}$), the weaker band not being observed. The molar conductivity for $[Co_2L1Cl_2](ClO_4)_2$ (**7**) in DMF suggests that the chloride anions remain bound. Therefore, this chloride derivative can potentially exist in solution (at room temperature) as either a high-spin square pyramidal or high-spin octahedral (with coordinated chloride anions and/or DMF and/or water molecules) complex. Axially compressed octahedral Co(II) systems often have broad ill-defined UV-Visible spectra.[25–27] The observation of one weak broad band centred at 1075 nm (ε = 27 $dm^3\ mol^{-1}\ cm^{-1}$) with a width of ~300 nm is consistent with this assignment for **7**.

The FAB mass spectra of these complexes show similar fragmentation patterns which are associated with the successive loss of their respective anions. $[Co_2L1(MeCN)_4](ClO_4)_4$ (**1**·4MeCN), $[Co_2L1(H_2O)_4](ClO_4)_4$ (**2**) and $[Co_2L1Cl_2](ClO_4)_2$ (**7**) share a common peak at *m*/*z* 565 due to the fragment $[Co_2L1](ClO_4)^+$. The very limited solubility of $[Co_2L1(NCS)_2(SCN)_2]$ (**6**) was nevertheless sufficient to record the mass spectrum. A strong peak at *m*/*z* 466, corresponding to $[Co_2L1]^+$, is common to all spectra, including that of **7**. The mass spectrum of **7** indicates that changes do occur in the coordination sphere of the cobalt centres in DMF solution; specifically, there is a strong peak at *m*/*z* 644 that is consistent with the presence of $[Co_2L1Cl_3(DMF)]^+$.

Electron paramagnetic resonance spectra were recorded for **7** in DMF as a frozen glass, $[Co_2L1(MeCN)_4](ClO_4)_4$ (**1**·4MeCN) and $[Co_2L1(NCO)_3]ClO_4$ (**5**) in acetonitrile as frozen glasses, and $[Co_2L1(NCS)_2(SCN)_2]$ (**6**) as a powdered sample at 77 K (Fig. 2). The line shapes are due to monomer impurities and not to the dinuclear parent, for which $\Delta m_s = \pm 1$ and ± 2 transitions would be expected.[28] The EPR spectrum of $[Co_2L1Cl_2](ClO_4)_2$ (**7**) is consistent with the presence of an axially-contracted

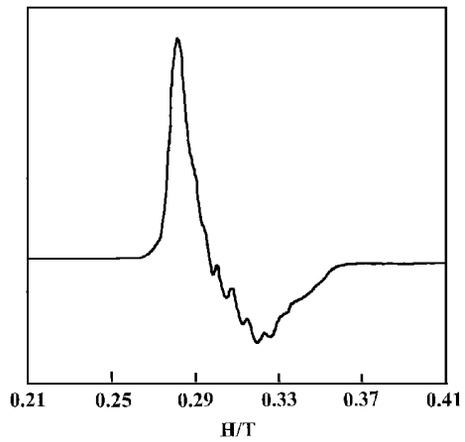

Fig. 2 X-Band EPR spectrum of $[Co_2L1(MeCN)_4](ClO_4)_4$ (**1**·4MeCN) in frozen MeCN.

low-spin octahedral Co(II) complex [$g_\perp = 2.08$, $g_\parallel = 2.30$ ($A_\parallel$ = 60 G)] (and another unidentified species, presumably a breakdown product). The EPR spectrum of **1**·4MeCN is similar. However, this time the spectrum is characteristic of an axially-extended low-spin octahedral complex [$g_\perp = 2.27$, $g_\parallel = 2.03$ ($A_\parallel$ = 60 G)].[26,27,29] Both EPR spectra are consistent with the solid state variable temperature magnetic moment data, which show that these two complexes possess low-spin Co^{II} centres at these low temperatures (1.46 BM per Co at 183 K and 1.90 BM per Co at 139 K, respectively). Due to the insoluble nature of $[Co_2L1(NCS)_2(SCN)_2]$, the EPR spectrum was obtained on the powdered solid (g = 2.14 at 77 K) and confirmed the g value obtained from the fit of the magnetic data. Consistent with the variable temperature magnetic data (~4.5 BM per Co from 100 to 300 K, HS), the EPR spectrum of the complex $[Co_2L1(NCO)_3]ClO_4$ in acetonitrile at 139 K gave no signal over this range, 4 K would be required to observe any high-spin signal. As indicated above, all of these comments on the observed EPR signals refer to their origin from monomeric Co(II) S = 1/2 impurities, and these aid in assigning geometries in the corresponding dinuclear species. Ideally, EPR studies of Co(II)-doped dinuclear zinc(II) complexes would help identify the single-ion Co(II) behaviour.

X-Ray crystal structures

Orange crystals of $[Co_2L1(H_2O)_4](ClO_4)_4·2H_2O·2MeCN$ (**2**·$2H_2O·2MeCN$) suitable for X-ray diffraction studies were grown by the slow diffusion of diethyl ether vapour into an acetonitrile solution of $[Co_2L1](ClO_4)_4$ containing 9% water and the crystal structure determined (Fig. 3, Table 1). The

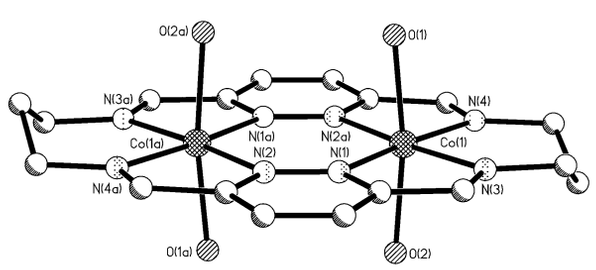

Fig. 3 Perspective view of the cation of **2**, $[Co_2L1(H_2O)_4]^{4+}$ (hydrogen atoms omitted for clarity). Symmetry operation: a $-x$, $1-y$, $-z$.

asymmetric unit consists of one half of the complex, with the other half generated by inversion. Both cobalt(II) centres are in a distorted octahedral environment, with angles subtended at the cobalt(II) centres varying from 76.64(17)–110.62(16)°. The six donors consist of four nitrogen donors (comprised of two pyridazine and two imine donors from the macrocycle) and two oxygen atoms from two coordinated water molecules. The Co–N(pyridazine) bond distances are on average 0.050(4) Å longer then the Co–N(imine) bonds. The Co(1) atom sits almost exactly in the N_4 basal plane, with only a minute shift towards O(2) [0.004(2) Å]. There is an extensive hydrogen-bonding network between the water molecules coordinated to the cobalt ions, the perchlorate anions and the various solvent molecules present in the unit cell.

Orange single crystals of $[Co_2L1(H_2O)_4](S_2O_6)_2·4H_2O$, the hydrated analogue of **3**, suitable for X-ray diffraction studies were grown by the slow diffusion of tetrahydrofuran vapour into a water solution of $[Co_2L1](S_2O_6)_2$. The structure was determined (Fig. 4 and Table 1) and demonstrates the non-

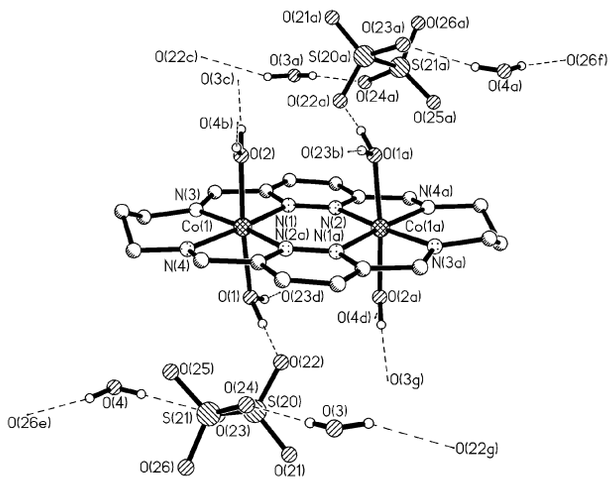

Fig. 4 Perspective view of **3**·$8H_2O$, $[Co_2L1(H_2O)_4](S_2O_6)_2·4H_2O$, showing the hydrogen-bonding network (only the hydrogen atoms in the water molecules are shown). Symmetry operations: a $1-x$, $2-y$, $1-z$; b $x-1$, y, z; c x, y, $z-1$; d $2-x$, $2-y$, $1-z$; e $2-x$, $1-y$, $2-z$; f $x-1$, $y+1$, $z-1$; g $1-x$, $2-y$, $2-z$.

coordinating nature of the dithionate anions, such that the structure is very similar to that of **2**·$2H_2O·2MeCN$ (Fig. 3). The asymmetric unit consists of one half of the complex, with the other half generated by inversion. Both cobalt(II) centres are in a distorted octahedral environment, with angles subtended at the cobalt(II) centres varying from 76.89(7)–110.03(6)°. The six donors consist of four nitrogen donors (comprised of two pyridazine and two imine donors from the macrocycle) and two oxygen atoms from two coordinated water molecules. The Co–N(pyridazine) bond distances are, on average, 0.0422(16) Å longer then the Co–N(imine) bonds. The Co(1) atom is further removed from the N_4 basal plane than in **2**·$2H_2O·2MeCN$, with a shift towards O(1) of 0.1642(24) Å. All hydrogen atoms of the coordinated and uncoordinated water molecules are involved in an extensive hydrogen-bonding network with the dithionate anions (Fig. 4).

Orange crystals of $[Co_2L1(NCO)_3]ClO_4$ (**5**), marginally suitable for X-ray diffraction studies, were grown by the slow diffusion of diethyl ether vapour into an acetonitrile solution and the X-ray crystal structure determined (Fig. 5). The asymmetric unit consists of one half of the complex, with the other half generated by a mirror plane. Unfortunately, due to the poor quality of the crystal ($R1$ = 0.15), a meaningful analysis of bond lengths and angles is not possible, however the overall structure of the complex is perfectly clear (Fig. 5). Whilst the bowed shape of the ligand L1 is unusual, it has been observed before for the manganese(II) thiocyanate complex of L1.[2]

The structures of **1**·4MeCN and the tetrathiocyanate derivative **6** have been reported previously.[4,5] To date, single crystals of the diazide derivative, **4**, have eluded us: twinning has been a recurring problem. However, from the magnetic data (*vide infra*) the complex is expected to have the flat L1 macrocycle conformation observed for **2**. The dichloride derivative, **7**, has, with

Table 1 Selected bond lengths (Å) and angles (°) for $[Co_2L1(MeCN)_4](ClO_4)_4$ (**1**·4MeCN), $[Co_2L1(H_2O)_4](ClO_4)_4·2H_2O·2MeCN$ (**2**·$2H_2O$·2MeCN), $[Co_2L1(H_2O)_4](S_2O_6)_2·4H_2O$ (**3**·$8H_2O$) and $[Co_2L1(NCS)_2(SCN)_2]$ (**6**)

	1·4MeCN	**2**·$2H_2O$·2MeCN	**3**·$8H_2O$	**6**
Co(1)–N(1)	2.013(4)	2.127(4)	2.1264(16)	1.966(3)
Co(1)–N(2a)[a]	2.005(4)	2.125(4)	2.1245(16)	1.983(3)
Co(1)–N(3)	1.948(4)	2.080(4)	2.0828(17)	1.933(3)
Co(1)–N(4)	1.964(4)	2.085(5)	2.0837(17)	1.922(3)
Co(1)–N(20)	2.135(4)			2.115(3)
Co(1)–S(30)				2.5843(10)
Co(1)–N(30)	2.127(4)			
Co(1)–O(1)		2.068(4)	2.0825(15)	
Co(1)–O(2)		2.079(4)	2.0564(16)	
N(1)–Co(1)–N(2a)[a]	103.7(2)	110.62(16)	110.03(6)	102.19(11)
N(1)–Co(1)–N(3)	80.8(2)	76.64(17)	76.89(7)	82.07(11)
N(3)–Co(1)–N(4)	94.3(2)	96.04(18)	96.03(7)	93.80(12)
N(2a)–Co(1)–N(4)[a]	81.2(2)	76.70(18)	77.04(6)	81.94(11)
N(1)–Co(1)–N(20)	92.1(2)			91.21(11)
N(2a)–Co(1)–N(20)[a]	85.9(2)			92.76(11)
N(3)–Co(1)–N(20)	93.7(2)			90.28(12)
N(4)–Co(1)–N(20)	90.3(2)			88.56(12)
N(1)–Co(1)–S(30)				92.69(8)
N(2a)–Co(1)–S(30)[a]				86.80(8)
N(3)–Co(1)–S(30)				89.87(9)
N(4)–Co(1)–S(30)				87.49(9)
N(1)–Co(1)–N(30)	89.4(2)			
N(2a)–Co(1)–N(30)[a]	87.6(2)			
N(3)–Co(1)–N(30)	92.8(2)			
N(4)–Co(1)–N(30)	88.8(2)			
N(1)–Co(1)–O(1)		86.38(16)	88.32(6)	
N(2a)–Co(1)–O(1)[a]		87.00(16)	87.29(6)	
N(3)–Co(1)–O(1)		93.38(17)	92.61(6)	
N(4)–Co(1)–O(1)		93.95(18)	91.37(6)	
N(1)–Co(1)–O(2)		87.60(16)	89.89(6)	
N(2a)–Co(1)–O(2)[a]		89.33(16)	88.89(6)	
N(3)–Co(1)–O(2)		91.24(17)	91.58(7)	
N(4)–Co(1)–O(2)		92.80(18)	90.98(7)	

[a] Symmetry operation a for: **1**·4MeCN is $1 - x, 1 - y, 1 - z$; **2**·$2H_2O$·2MeCN is $-x, 1 - y, - z$; **3**·$8H_2O$ is $1 - x, 2 - y, 1 - z$; **6** is $-x, -y, -z$.

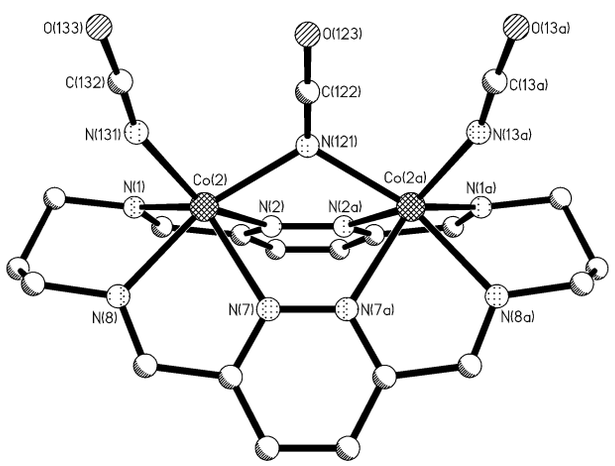

Fig. 5 Perspective view of the cation of **5**, $[Co_2L1(NCO)_3]^+$ (hydrogen atoms omitted for clarity).

one exception, formed powders from all solvent combinations tried. The exception occurred in an attempt to recrystallise a sample from dry DMF by diethyl ether vapour diffusion, but the crystals were tiny and larger ones have not been forthcoming, to date. By analogy with the dicopper(II) complex $[Cu_2L1Cl_2](ClO_4)_2$, in the solid state, complex **7** is expected to have a fairly flat L1 conformation with the chloride ions coordinated to the axial sites of the cobalt(II) ions, making them square pyramidal: a weak intermolecular "ladder" stacking interaction may exist.[7]

The X-ray structural determinations for the complexes $[Co_2L1(H_2O)_4]^{4+}$ (as both perchlorate **2** and dithionate **3** salts), $[Co_2L1(MeCN)_4]^{4+}$ and $[Co_2L1(NCS)_2(SCN)_2]$ have all been obtained at similar temperatures (158, 163, 170 and 163 K, respectively). Also, the magnetic moment data (*vide infra*) have shown $[Co_2L1(H_2O)_4]^{4+}$ to be high spin (3.88 BM per Co for **2**, 4.00 BM per Co for **3**), $[Co_2L1(MeCN)_4]^{4+}$ to be predominantly low spin (2.08 BM per Co) and $[Co_2L1(NCS)_2(SCN)_2]$ to be low spin (1.92 BM per Co) at these temperatures. Therefore, a comparison of bond lengths and angles has been undertaken to correlate the spin states with these structural parameters. Examination of the bond lengths for these four complexes (Table 1) shows that, in all cases, regardless of spin state, significantly longer bond distances are observed for the Co–N(pyridazine) bonds than for the Co–N(imine) bonds. This is also apparent in the analogous dicopper(II) complexes.[3,7]

Examination of the bond length differences between the axial and in-plane donors of each complex reveals that axially-extended nitrogen donors are observed for both the $[Co_2L1(MeCN)_4]^{4+}$ and $[Co_2L1(NCS)_2(SCN)_2]$ complexes. This has subsequently been confirmed for $[Co_2L1(MeCN)_4]^{4+}$ *via* EPR, although admittedly at a higher temperature (see above). The donors for the high-spin complexes $[Co_2L1(H_2O)_4]^{4+}$ (**2** and **3**) do not show axial extension: the Co–O(axial) bond lengths are of similar length to the Co–N(imine) distances. Finally, a clear trend of shortening of the Co–N(L1) bond distances can be seen on going from $[Co_2L1(H_2O)_4]^{4+}$ (HS) to $[Co_2L1(MeCN)_4]^{4+}$ (predominantly LS) to $[Co_2L1(NCS)_2(SCN)_2]$ (LS), as expected.

A clear trend can also be ascertained from a comparison of the donor–Co–donor angles (Table 1). On going from $[Co_2L1(H_2O)_4]^{4+}$ (HS) to $[Co_2L1(MeCN)_4]^{4+}$ (predominantly LS) to $[Co_2L1(NCS)_2(SCN)_2]$ (LS) both the N(L1)–Co–N(L1) angles and the axial donor–Co–axial donor angles tend toward the octahedral donor angle of 90° {N(L1)–Co–N(L1) angles: $[Co_2L1(H_2O)_4]^{4+}$ 76.6–110.6°, $[Co_2L1(MeCN)_4]^{4+}$ 80.8–103.7°,

Table 2 Magnetic parameters for the $\{Co^{II}_2L1\}^{4+}$ complexes obtained using isotropic $-2J\mathbf{S_1}\cdot\mathbf{S_2}$ models

Compound no.	Complex	S_{Co}	$2J$ (± 0.1)/cm^{-1}	g (± 0.02)	ρ^a (± 0.005)
1	$[Co_2L1](ClO_4)_4$ [b]	1/2	−10.2	2.13	0.01
1·4MeCN	$[Co_2L1(MeCN)_4](ClO_4)_4$ [b]	1/2	−14.2	2.15	0.01
2	$[Co_2L1(H_2O)_4](ClO_4)_4$	3/2	−19.2	2.05	0.03
3·8H_2O	$[Co_2L1(H_2O)_4](S_2O_6)_2\cdot4H_2O$	3/2	−20.2	2.35	0.03
4	$[Co_2L1(N_3)_2](ClO_4)_2$	3/2	−20.5	2.25	0.02
5	$[Co_2L1(NCO)_3]ClO_4$	3/2	−7.5	2.42	0.01
6	$[Co_2L1(NCS)_2(SCN)_2]$ [b]	1/2	−11.7	2.13	0.00
7	$[Co_2L1Cl_2](ClO_4)_2$ [c]	1/2	*ca.* −66	1.94	0.01

[a] Fraction monomer. [b] Only the low-spin (S = 1/2, S = 1/2) region of these spin-crossover species are fitted. [c] See text re. poor fit.

$[Co_2L1(NCS)_2(SCN)_2]$ 81.9–102.2°. Axial donor–Co–axial donor angles: $[Co_2L1(H_2O)_4]^{4+}$ 86.4–94.0°, $[Co_2L1(MeCN)_4]^{4+}$ 85.9–93.7°, $[Co_2L1(NCS)_2(SCN)_2]$ 86.8–92.8°}.[30]

Magnetochemistry

Variable temperature magnetic susceptibility measurements were made on powdered samples of **1**–**7** and **1**·4MeCN in the temperature range 320 to 4.2 K.

The magnetic susceptibility data for the four high-spin complexes $[Co_2L1(H_2O)_4](ClO_4)_4$ (**2**), $[Co_2L1(H_2O)_4](S_2O_6)_2\cdot4H_2O$ (**3**·8H_2O), $[Co_2L1(N_3)_2](ClO_4)_4$ (**4**) and $[Co_2L1(NCO)_3]ClO_4$ (**5**) were observed to gradually increase as the temperature was decreased from 300 K, reaching a maximum at ~50 K before decreasing sharply at lower temperatures (Fig. 6). The

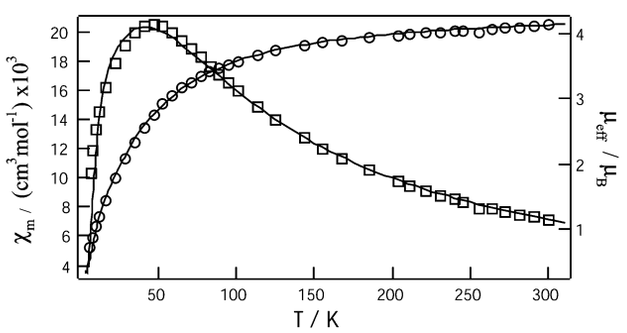

Fig. 6 Experimental temperature dependence of χ_M (□) and μ (○), per Co, for $[Co_2L1(H_2O)_4](ClO_4)_4$ (**2**). The solid lines are the calculated fit of the data to a S = 3/2 isotropic Heisenberg model: $2J = -19.2$ cm^{-1}, $g \approx 2.05$.

corresponding values of magnetic moment remained approximately constant on decreasing the temperature from 300 to 100 K, but below 100 K the values decreased rapidly towards zero (Fig. 6). This behaviour is typical of high-spin (S = 3/2) dinuclear cobalt(II) complexes exhibiting weak antiferromagnetic exchange. In contrast, mononuclear high-spin Co(II) compounds do not show maxima in susceptibilities and the μ values change with temperature but do not decrease to zero at low temperatures. The susceptibility data were fitted to a simple S = 3/2 dimer isotropic Heisenberg ($-2J\mathbf{S_1}\cdot\mathbf{S_2}$) model. This model makes significant approximations and assumes no orbital degeneracy on the distorted octahedral Co(II) ($^4T_{1g}$) centres and zero-field splitting effects are ignored.[31–33]

The best fit parameters are given in Table 2. Despite the approximations alluded to above, the J values are reasonably indicative of the exchange interactions across the pyridazine bridges. The high values of g for the cyanate and azide derivatives reflect the spin–orbit coupling effects and orbital degeneracy of octahedral Co(II).[32,33] The 2J values for the aqua and azide adducts are *ca.* −20 cm^{-1}, with the corresponding value for the cyanate complex being much smaller (−7.5 cm^{-1}) and the χ_{max} shape being narrower than in Fig. 6. This difference in 2J relates to the markedly different cobalt and ligand geometries noted for $[Co_2L1(NCO)_3]ClO_4$ (**5**) as compared to $[Co_2L1(H_2O)_4](ClO_4)_4$ (**2**) (Fig. 3 and 4). In contrast, the similarity of the 2J values for $[Co_2L1(H_2O)_4](ClO_4)_4$ (**2**), $[Co_2L1(H_2O)_4](S_2O_6)_2\cdot4H_2O$ (**3**·8H_2O) and $[Co_2L1(N_3)_2](ClO_4)_2$ (**4**) indicates that the conformation of L1 in **4** is similar to that found in the structurally characterised complexes **2** and **3**.

The magnetic susceptibility data for the complex $[Co_2L1Cl_2](ClO_4)_2$ (**7**) increased gradually as the temperature decreased from 300 to 50 K, before rising more rapidly,probably due to small amounts of monomeric impurity. The corresponding values of the magnetic moment decreased with decreasing temperature, from 1.62 μ_B at 300 K to 0.64 μ_B at 4.2 K. This behaviour is that anticipated for a low-spin (S = 1/2) cobalt(II) dimer with moderate antiferromagnetic exchange, except that the expected maximum in χ was not observed. The EPR data confirm the low-spin character of the monomeric impurity in this chloride complex in the solid state and at low temperature in DMF. The temperature dependence of the molar magnetic susceptibilities of an isolated dinuclear low-spin cobalt(II) complex [assuming orbital contributions on Co(II) are neglected] is expected to obey the Bleaney–Bowers equation for an S = 1/2 dimer, which is based on an isotropic $-2J\mathbf{S_1}\cdot\mathbf{S_2}$ Hamiltonian.[34] It was possible to get a rough fit to the susceptibility data in the range 50–300 K with $2J \approx -66$ cm^{-1} and g = 1.94, the g value being well below that deduced from the EPR spectra (g = 2.15). The data at < 50 K could not be reproduced by incorporating a fraction of monomer, without losing agreement at > 50 K. Further work is required on the magnetism and structure of this chloro-complex which probably has a polymeric 'ladder' structure, as in the copper(II) analogue.[7]

The complexes $[Co_2L1](ClO_4)_4$ (**1**), $[Co_2L1(MeCN)_4](ClO_4)_4$ (**1**·4MeCN) and $[Co_2L1(NCS)_2(SCN)_2]$ (**6**) exhibit very interesting magnetochemistry. The data for **6** have been discussed in a preliminary paper.[5] The magnetic susceptibility data for **1**·4MeCN and **6** decreased gradually from 300 K to shallow minima at 240 and 210 K, respectively, before rising to a sharp maximum at 10 K and dropping rapidly at temperatures below this (Fig. 7). The observed molar susceptibility of **1** was quite similar, except that the shallow minimum was not present. The corresponding values of the magnetic moments for **1**·4MeCN

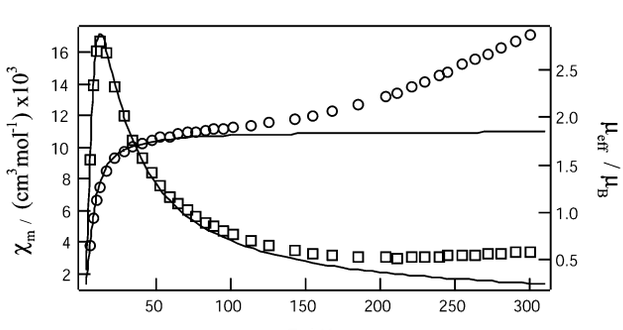

Fig. 7 Experimental temperature dependence of χ_M (□) and μ (○), per Co, for $[Co_2L1(MeCN)_4](ClO_4)_4$ (**1**·4MeCN). The solid lines are the calculated fit of the data to a S = 1/2 dimer model: $2J = -14.2$ cm^{-1}, g = 2.15, fraction monomer 0.01.

and **6** decreased with decreasing temperature, at first relatively steeply from 300 K down to 150 K and 220 K, respectively, then more gradually to ~40 K and finally a rapid decrease was observed at temperatures below this. The corresponding values of the magnetic moment for **1** were similar to those observed for the acetonitrile-bound complex, but the initial decrease was considerably more gradual. When the isotropic $S = 1/2$ dimer model was used to model the observed behaviour, satisfactory fits for the three complexes were obtained at low temperatures, in the region of the susceptibility maximum. The higher temperature regions show deviations because of the influence of the high-spin Co(II) state. The best-fit magnetic parameters are given in Table 2. The *g* values are typical of low-spin Co(II), that for **1**·4MeCN agreeing well with the EPR *g* value (2.11). The 2*J* values are in the range -10 to -15 cm^{-1}. The magnetic moment plots above 200 K for **1**·4MeCN and **6** are consistent with a gradual spin transition which is incomplete at the high temperature end. No hysteresis effects were observed in these spin-crossover regions. In the case of **6**, the $S = 3/2$ state of each Co(II) ion is not fully populated at 350 K and the transition is expected to plateau at ~4.2 BM, based on related monomeric $S = 3/2$ complexes.[32,35] These two complexes represent the first examples of dimetallic cobalt(II) complexes which exhibit the spin-crossover phenomenon. The magnetic moment data for **1** is similar, but considerably less pronounced and while this may also be due to a small degree of spin-crossover, it may also be due to orbital degeneracy (spin–orbit coupling effects), which is not included in the model used to fit the data.

In all of the above examples, weak antiferromagnetic exchange, *via* the double pyridazine bridge, is observed. The overlap between the Co(II) $d_{x^2-y^2}$ magnetic orbital and the pyridazine nitrogen p orbitals is the important factor affecting the size of the exchange integral in the high-spin examples. The observation that the magnetic exchange of the bent complex $[Co_2L1(NCO)_3]ClO_4$ is smaller than that of the other co-planar examples is consistent with this. The magnitude of the antiferromagnetic exchange of these complexes ($2J = -7.5$ to -20 cm^{-1}) correlates well to the few other dicobalt double pyridazine-bridged complexes reported ($2J = -23$ to -29.4 cm^{-1})[16,17,19] and to a related triazole-bridged complex ($2J = -8$ cm^{-1}).[36]

Comparison of these dicobalt(II) complexes with our recently reported dicopper(II) doubly-bridged pyridazine complexes[3,6,7] shows a total energy spread for Co(II) (12*J*) of *ca.* -240 cm^{-1} and for Cu(II) (2*J*) of *ca.* -480 cm^{-1}. The square pyramidal dicopper(II) complexes of L1, both free of acetonitrile and also with coordinated NCS^- ions and water molecules, all exhibit antiferromagnetic exchange approximately twice as strong as the similar derivatives containing dicobalt(II) ions. A comparison of the structurally characterised complexes, $[Cu_2L1(MeCN)_2](ClO_4)_4$ (**8**) and $[Cu_2L1(H_2O)_2](ClO_4)_4$ (**9**) with the analogous cobalt complexes $[Co_2L1(MeCN)_4](ClO_4)_4$ and $[Co_2L1(H_2O)_4](ClO_4)_4$ shows remarkable similarities between the M–N(L1) bond lengths [1.96–2.04 for **8**; 1.99–2.06 for **9**; 1.95–2.01 for **1**·4MeCN; 2.08–2.13 for **2**·2H$_2$O·2MeCN; 2.08–2.13 Å for **3**], M ··· M separations [3.805 for **8**; 3.888 for **9**; 3.807, 3.809 for **1**·4MeCN; 3.750 for **2**·2H$_2$O·2MeCN; 3.769 Å for **3**] and the M–N(pyr)–N(pyr) angles [129.3(2), 128.4(2) for **8**; 128.3(6), 129.2(6) for **9**; 128.0(3), 128.3(3), 128.6(3), 128.5(3) for **1**·4MeCN; 124.9(3), 124.4(3) for **2**·2H$_2$O·2MeCN; 124.9(1), 124.8(1)° for **3**] of the low-spin, as opposed to high-spin, cobalt(II) complex and the copper complexes. Glerup *et al.*[33] have compared *J* values for a series of μ-oxalato-bridged complexes (M^{II} = Mn, Fe, Co, Ni, Cu) and found a good correlation for Mn to Ni, with 2*J* values calculated using a model involving charge-transfer states. However, the Cu^{II} system did not fit the trend in 2*J* values because it did not use a $d_{x^2-y^2}$ magnetic orbital. This is probably the reason that the present Co^{II} $S = 1/2$ compounds **1**, **1**·4MeCN and **6** have such low 2*J* values in comparison to the Cu^{II} compounds, a situation supported by EPR for **1**·4MeCN.

Conclusions

Prior to this research program, few pyridazine or phthalazine-bridged dicobalt(II) macrocyclic complexes were known. Here, we have described the synthesis, structure and magnetic properties of a series of such complexes derived from $[Co_2L1](ClO_4)_4$ (**1**). These provide a rare example of a range of complexes derived from a common ligand, yet spanning the range of high-spin (**2**–**5**) to spin-crossover (**1**·4MeCN, **6**) to low-spin (**7**) complexes, simply by appropriate choice of axial ligand. The X-ray structure determinations of $[Co_2L1(H_2O)_4](ClO_4)_4$·2H$_2$O·2MeCN (**2**·2H$_2$O·2MeCN) and $[Co_2L1(H_2O)_4](S_2O_6)_2$·4H$_2$O (**3**·8H$_2$O) revealed almost planar macrocyclic complexes, with bond lengths to the octahedral cobalt centres characteristic of high-spin dicobalt(II) centres. This was confirmed by variable temperature magnetic susceptibility data. Unlike all of the other structurally characterised dicobalt complexes, in which an almost planar L1 conformation is observed, $[Co_2L1(NCO)_3]ClO_4$ (**5**) had a folded L1 conformation, a situation that has been observed only once before, for $[Mn_2L1(NCS)_4]$.[2] The variable temperature magnetic moment data showed this octahedral cobalt complex and the orange–brown complex $[Co_2L1(N_3)_2](ClO_4)_2$ (**4**) to be high spin. The purple–black complex $[Co_2L1Cl_2](ClO_4)_2$ (**7**) was shown to be low spin by variable temperature magnetic moment data. Both the dichloride and diazide complexes have resisted all attempts, to date, to structurally characterise them.

The variable temperature magnetic moment study on **1**·4MeCN and $[Co_2L1(NCS)_2(SCN)_2]$ (**6**) revealed the first examples of dicobalt complexes which exhibit both a LS ⇔ HS spin transition and exchange coupling.[5] Since our work commenced, there has been an upsurge of interest in binuclear Fe^{II}-Fe^{II} spin-crossover complexes, particularly those of the type $(NCS)_2$(chel)Fe(μ-bipyrimidine)Fe(chel)$(NCS)_2$, where chel = bithiazoline.[20,37] The interplay between spin crossover and magnetic exchange, the latter occurring across the bipyrimidine bridge, was investigated and pair spin states such as the LS–HS mixed-spin state were stabilised as a result of this interplay. However, the simultaneous observation of exchange and spin crossover in the susceptibility data, of the type observed here for **1**·4MeCN and **6**, was not detected directly. It remains to be seen what values of *J* will render HS–LS, HS–HS and LS–LS descriptions inoperable. At the moment, we have quantified the LS–LS coupling in the present $Co^{II}Co^{II}$ crossover species, but not the HS–LS and HS–HS regimes. However, the HS–HS coupling has been quantified in complexes **2**–**5**. In $Fe^{II}Fe^{II}$ crossover compounds, the LS–LS states, are, of course, diamagnetic. Interestingly, the analogous bipyrimidine-bridged $Co^{II}Co^{II}$ compounds, $(NCS)_2$(chel)Co(μ-bipyrimidine)Co(chel)$(NCS)_2$, with chel = bipyrimidine, showed only HS–HS coupled behaviour, and as in the $Fe^{II}Fe^{II}$ case (at atmospheric pressure), a similar small negative *J* value.[32] It would be interesting to explore the cobalt-μ-bipyrimidine system containing chel = bithiazoline for comparison with **1**·4MeCN and **6**.

Experimental

$[Pb_2(4 + 4)](ClO_4)_4$ was synthesised according to the literature preparation.[2] Acetonitrile was refluxed over calcium hydride and distilled prior to use. Dimethylformamide (DMF, spectroscopic grade) was stored over molecular sieves. Nitromethane (AR) was used as received.

CAUTION! Whilst no problems were encountered in the course of this work, perchlorate mixtures are potentially explosive and should therefore be handled with appropriate care.

Syntheses

$[Co_2L1](ClO_4)_4$ (1). To a refluxing fawn suspension of $Pb_2(4 + 4)(ClO_4)_4$ (0.374 g, 0.248 mmol) in dry acetonitrile (40 cm^3) was added dropwise $Co(ClO_4)_2$·6H$_2$O (0.368 g, 1.00 mmol) in

hot dry acetonitrile (10 cm^3). The resulting ruby-red solution was refluxed for 1 h. $[Co_2L1(MeCN)_4](ClO_4)_4$ was isolated as a dark red crystalline material by vapour diffusion of diethyl ether into the reaction mixture, and, on drying *in vacuo*, gave **1** (0.250 g, 57%). Found: C, 24.9; H, 2.6; N, 12.8; $C_{18}H_{20}N_8Cl_4O_{16}Co_2$ (**1**) requires: C, 25.0; H, 2.3; N, 13.0%. IR (KBr disk, *inter alia*) ν_{max}/cm^{-1}: 3418, 3067, 3011, 2948, 1642, 1580, 1551, 1440, 1350, 1098, 626. FAB *m*/*z* (fragment): 565 $([Co_2L1]ClO_4)^+$, 466 $([Co_2L1])^+$. Λ_m(MeCN) = 353 $cm^2\ mol^{-1}\ \Omega^{-1}$ (*c.f.* 340–420 for a 3 : 1 electrolyte in MeCN[24]). λ_{max}/nm (MeCN) ($\varepsilon/dm^3\ mol^{-1}\ cm^{-1}$): 354 (2727), 422 (3384), 536 (2809). λ/nm ($MeNO_2$) ($\varepsilon/dm^3\ mol^{-1}\ cm^{-1}$): *ca.* 390sh (*ca.* 1780), 466 (1530), *ca.* 525sh (*ca.* 1155), 850 (7). μ = 2.88 BM per Co (SQUID, 298 K, MeCN bound); μ = 2.38 BM per Co (SQUID, 298 K, MeCN free).

$[Co_2L1(H_2O)_4](ClO_4)_4$ (2). To a stirred deep red solution of **1** (0.086 g, 0.10 mmol) in dry acetonitrile (7 cm^3) was added a small aliquot of water (0.6 cm^3). The resulting bright orange solution was stirred for 10 min, then crystallised by slow diffusion of diethyl ether into the reaction solution to give orange single crystals of $[Co_2L1(H_2O)_4](ClO_4)_4\cdot 2H_2O\cdot 2MeCN$. These were filtered off and air dried to give $[Co_2L1(H_2O)_3(MeCN)](ClO_4)_4$ (0.065 g, 68%). Found: C, 25.3; H, 3.4; N, 12.9; $C_{18}H_{20}N_8Cl_4O_{16}Co_2\cdot 3H_2O\cdot MeCN$ requires: C, 25.0; H, 3.1; N, 13.1%. IR (KBr disk, *inter alia*) ν_{max}/cm^{-1}: 3441, 3071, 2933, 2871, 1655, 1602, 1588, 1554, 1448, 1348, 1102, 965, 884, 625. FAB *m*/*z* (fragment): 763 $([Co_2L1](ClO_4)_3)^+$, 664 $([Co_2L1](ClO_4)_2)^+$, 565 $([Co_2L1]ClO_4)^+$, 466 $([Co_2L1])^+$. $\Lambda_m(H_2O)$ = 398 $cm^2\ mol^{-1}\ \Omega^{-1}$. λ_{max}/nm (H_2O) ($\varepsilon/dm^3\ mol^{-1}\ cm^{-1}$): 358 (2250), 841 (9), 965 (6). μ = 3.82 BM per Co (SQUID, 298 K).

$[Co_2L1](S_2O_6)_2$ (3). Complex **1** (0.200 g, 0.23 mmol) was dissolved in hot water (15 cm^3) to give a deep orange solution. To this was added $Na_2S_2O_6\cdot 2H_2O$ (0.112 g, 0.46 mmol) in water (5 cm^3). The resulting solution was heated and stirred for 10 min, after which stirring was stopped and the solution left to cool to room temperature. The orange crystals which formed over the next 24 h were collected and recrystallised from hot water to give $[Co_2L1(H_2O)_4](S_2O_6)_2\cdot 4H_2O$ as orange crystals (0.083 g, 39%). Found: C, 23.34; H, 3.63; N, 12.48; S, 13.53; $C_{18}H_{20}N_8O_{12}S_4Co_2\cdot 8H_2O$ requires: C, 23.23; 3.90; N, 12.04; S, 13.78% After drying *in vacuo*, **3** was obtained as a powder (0.070 g, 39%). Found: C, 27.7; H, 2.7; N, 14.3; S, 16.4; $C_{18}H_{20}N_8O_{12}S_4Co_2$ requires: C, 27.5; H, 2.6; N, 14.3; S, 16.3%. IR (KBr disk, *inter alia*) ν_{max}/cm^{-1}: 3427, 3362, 3046, 3003, 2947, 1623, 1577, 1245, 991, 584, 514. $\Lambda_m(H_2O)$ = 270 $cm^2\ mol^{-1}\ \Omega^{-1}$. λ_{max}/nm (H_2O) ($\varepsilon/dm^3\ mol^{-1}\ cm^{-1}$): 359 (2450), 839 (18). μ = 4.10 BM per Co (SQUID, 298 K).

$[Co_2L1(N_3)_2](ClO_4)_2$ (4). Complex **1** (0.121 g, 0.14 mmol) was dissolved in water (30 cm^3) to give a deep orange solution. To this was added NaN_3 (0.019 g, 1.12 mmol) in water (2 cm^3). The resulting brown solution was stirred for 5 min and then left to stand for 24 h, during which time **4** precipitated out as orange–brown crystalline stars. These were filtered off and dried *in vacuo* (0.040 g, 49%). Found: C, 27.4; H, 2.9; N, 24.3; $C_{18}H_{20}N_{14}Cl_2O_8Co_2\cdot 2.5H_2O$ (**4**·$2.5H_2O$) requires: C, 27.2; H, 3.2; N, 24.7%. IR (KBr disk, *inter alia*) ν_{max}/cm^{-1}: 3420, 3075, 2921, 2854, 2033, 1653, 1624, 1560, 1382, 1285, 1082, 625. FAB *m*/*z* (fragment): 554w $([Co_2L1(N_3)_2])^+$, 466 $([Co_2L1])^+$. Λ_m(MeCN) = 312 $cm^2\ mol^{-1}\ \Omega^{-1}$ (*c.f.* 220–300 for a 2 : 1 electrolyte in MeCN[24]). λ_{max}/nm (MeCN) ($\varepsilon/dm^3\ mol^{-1}\ cm^{-1}$): 365 (1816). μ = 4.05 BM per Co (SQUID, 298 K).

$[Co_2L1(NCO)_3]ClO_4$ (5). To a stirred deep red solution of **1** (0.300 g, 0.35 mmol) in dry acetonitrile (240 cm^3) was added solid NaOCN (0.067 g, 1.04 mmol). The resulting mixture was left to stir for 14 h, during which time the sodium cyanate dissolved and the solution colour changed from deep red to orange. Bright orange single crystals of **5** formed by the slow diffusion of diethyl ether into the reaction solution, were filtered off and dried *in vacuo* (0.127 g, 53%). Found: C, 36.4; H, 2.8; N, 22.4; $C_{21}H_{20}N_{11}ClO_7Co_2$ (**5**) requires: C, 36.5; H, 2.9; N, 22.3%. IR (KBr disk, *inter alia*) ν_{max}/cm^{-1}: 3490, 3056, 2949, 2923, 2864, 2196, 2155, 1648, 1641, 1580, 1556, 1450, 1320, 1120, 1086, 897, 623. FAB *m*/*z* (fragment): 649w $([Co_2L1(NCO)_2]ClO_4)^+$, 592w $([Co_2L1(NCO)_3])^+$, 550w $([Co_2L1(NCO)_2])^+$, 508w $([Co_2L1NCO])^+$, 466 $([Co_2L1])^+$. Λ_m(MeCN) = 129 $cm^2\ mol^{-1}\ \Omega^{-1}$ (*c.f.* 120–160 for a 1 : 1 electrolyte in MeCN[24]). λ_{max}/nm (MeCN) ($\varepsilon/dm^3\ mol^{-1}\ cm^{-1}$): 396 (3548), 918 (11). μ = 4.52 BM per Co (SQUID, 298 K).

$[Co_2L1(NCS)_2(SCN)_2]$ (6). Black single crystal cubes of **6**.[5] IR (KBr disk, *inter alia*) ν_{max}/cm^{-1}: 3038, 2925, 2074, 1624, 1569, 1415, 1317, 1117, 919, 886, 668. FAB *m*/*z* (fragment): 582 $([Co_2L1(SCN)_2])^+$, 524 $([Co_2L1(SCN)])^+$, 466 $([Co_2L1])^+$. λ_{max}(reflectance)/nm: *ca.* 370, 500, 630. μ = 0.7 BM per Co (SQUID, 4.5 K); μ = 3.2 BM per Co (SQUID, 350 K).

$[Co_2L1Cl_2](ClO_4)_2$ (7). Complex **1** (0.086 g, 0.10 mmol) was dissolved in dry acetonitrile (30 cm^3). To this was added $Et_4NCl\cdot H_2O$ (0.037 g, 0.20 mmol) in dry acetonitrile (2 cm^3). The resulting brown solution was stirred overnight, during which time **7** precipitated out as a deep purple–black powder, which was filtered off and dried *in vacuo* (0.056 g, 78%). Subsequent recrystallisation from dry DMF by the slow diffusion of diethyl ether gave $[Co_2L1Cl_2](ClO_4)_2\cdot H_2O$ as dark purple micro needles. Found: C, 28.7; H, 3.0; N, 14.8; $C_{18}H_{20}N_8Cl_4O_8Co_2\cdot H_2O$ (**7**·H_2O) requires: C, 28.7; H, 2.9; N, 14.9%. IR (KBr disk, *inter alia*) ν_{max}/cm^{-1}: 3503, 3062, 2956, 1653, 1602, 1580, 1422, 1323, 1117, 1079, 938, 627. FAB *m*/*z* (fragment): 644 $([Co_2L1Cl_3(DMF)])^+$, 600w $([Co_2L1Cl]ClO_4)^+$, 565 $([Co_2L1]ClO_4)^+$, 501w $([Co_2L1Cl])^+$, 466 $([Co_2L1])^+$. Λ_m(DMF) = 107 $cm^2\ mol^{-1}\ \Omega^{-1}$ (*c.f.* 130–170 for a 2 : 1 electrolyte in DMF[24]). λ_{max}/nm (DMF) ($\varepsilon/dm^3\ mol^{-1}\ cm^{-1}$): 407 (1989), 1075 (27). μ = 1.62 BM per Co (SQUID, 298 K).

X-Ray crystallography

Crystal data for $[Co_2L1(H_2O)_4](ClO_4)_4\cdot 2H_2O\cdot 2MeCN$ (2·$2H_2O\cdot 2MeCN$). $C_{22}H_{38}N_{10}O_{22}Cl_4Co_2$, orange plate, dimensions 0.45 × 0.14 × 0.08 mm, triclinic, space group $P\bar{1}$, a = 8.8623(16), b = 10.5945(19), c = 11.653(2) Å, β = 85.619(2)°, U = 1020.1(3) $Å^3$, μ = 1.168 mm^{-1}, Z = 1, D_c = 1.716 g cm^{-3}, $F(000)$ = 538, T = 158 K. 11856 reflections were collected using a Bruker SMART diffractometer and a semi-empirical absorption correction (SADABS) was applied (T_{min} = 0.77, T_{max} = 1.00). The 3947 independent reflections were used to solve the structure by direct methods (SHELXS86).[38,39] The refinement (SHELXL97)[40] of 271 parameters converged to $R1$ = 0.0675 [for 3277 reflections having $F > 4\sigma(F)$], $wR2$ = 0.1787 and GOF 1.082 (for all 3947 F^2 data), with all non-hydrogen atoms anisotropic, hydrogen atoms inserted at calculated positions with the exception of those on oxygen atoms O1 and O2 where they were located from difference maps and then moved along the vector to give an O–H bond length of 0.85 Å; peak/hole 1.49/−0.76 e $Å^{-3}$.

Crystal data for $[Co_2L1(H_2O)_4](S_2O_6)_2\cdot 4H_2O$ (3·$8H_2O$). $C_{18}H_{36}N_8O_{20}S_4Co_2$, orange rectangular prism, dimensions 0.75 × 0.38 × 0.15 mm, triclinic, space group $P\bar{1}$, a = 8.285(3), b = 10.959(3), c = 11.605(4) Å, β = 69.945(4)°, U = 886.0(5) $Å^3$, μ = 1.262 mm^{-1}, Z = 1, D_c = 1.744 g cm^{-3}, $F(000)$ = 478, T = 163 K. 11375 reflections were collected on a Bruker SMART diffractometer and a semi-empirical absorption correction (SADABS) was applied (T_{min} = 0.81, T_{max} = 1.00). The 3716 independent reflections were used to solve the structure by direct methods (SHELXS86).[38,39] The refinement (SHELXL97)[40] of 235 parameters converged to $R1$ = 0.0285 [for 3426 reflections having $F > 4\sigma(F)$], $wR2$ = 0.0776 and GOF 1.055 (for all 3716 F^2 data), with all non-hydrogen atoms anisotropic,

hydrogen atoms inserted at calculated positions with the exception of the hydrogen atoms on the water oxygen atoms which were located from difference maps and were allowed to ride on the attached atoms during the refinement; peak/hole 0.778/ −0.581 e Å^{-3}.

Crystal data for $[Co_2L1(NCO)_3]ClO_4$ (5). $C_{21}H_{20}N_{11}O_7ClCo_2$, orange rod, dimensions 0.38 × 0.18 × 0.13 mm, monoclinic, space group $C2/m$, a = 10.225(8), b = 22.34(2), c = 11.066(9) Å, β = 98.84(4)°, U = 2497(4) Å^3, μ = 1.505 mm^{-1}, Z = 4, D_c = 1.840 g cm^{-3}, $F(000)$ = 1400, T = 158 K. 1880 reflections were collected using a Bruker four-circle diffractometer and a semi-empirical absorption correction (SADABS) was applied. The 1619 independent reflections were used to solve the structure by direct methods (SHELXS86).[38,39] The refinement (SHELXL97)[40] of 195 parameters only converged (for details please see the CIF file) to $R1 = 0.147$ [for 1469 reflections having $F > 4\sigma(F)$], $wR2 = 0.333$ and GOF 1.128 (for all 1619 F^2 data) with all non-hydrogen atoms anisotropic; peak/hole 0.93/−1.19 e Å^{-3}.

CCDC reference numbers 175886, 175887 and 179659.

See http://www.rsc.org/suppdata/dt/b1/b111267h/ for crystallographic data in CIF or other electronic format.

Magnetic measurements

A Quantum Design MPMS5 SQUID magnetometer was used with an applied field of 1 T. In the case of complex **6** (see also ref. 5), the field was varied to 0.1 and 0.05 T, in the range 350–4.2 K, and the susceptibilities were identical. Samples were generally of mass *ca.* 20 mg and contained in gel capsules, except for those which readily lost solvent molecules (*eg.* MeCN); these were contained in a sealed quartz tube. The instrument was calibrated against a standard palladium sample and against $CuSO_4 \cdot 5H_2O$ and $[Ni(en)_3](S_2O_3)$. μ_{eff} values have estimated errors of ± 0.02 μ_B and temperatures ±0.05 K.

EPR spectra

X-Band spectra were measured from frozen solutions or neat powder samples using either a Varian E4 or E12 instrument, with typical instrumental settings being: microwave frequency 9.08 GHz, modulation frequency 100 KHz, modulation amplitude 20 G, microwave power 10 mV, time constant 0.25 sec, gain *ca.* 10^2.

Acknowledgements

This work was supported by grants from the University of Otago, the Marsden Fund (Royal Society of New Zealand) and the Australian Research Council. We are grateful to Professor W. T. Robinson and Dr J. Wikaira (University of Canterbury) for the X-ray data collections, B. M. Clark (University of Canterbury) for the FAB mass spectra and to M. Pahl (University of Otago) and Professor J. Nelson (Queens University, Belfast) for their help. S. B. thanks the University of Otago for granting study leave which facilitated the preparation of this manuscript, and gratefully acknowledges her hosts Professor M. D. Ward, Dr J. C. Jeffery and Professor J. McCleverty (Bristol University) and the financial support of a Royal Society of Chemistry Journals Grant.

References

1 S. Brooker, R. J. Kelly and G. M. Sheldrick, *J. Chem. Soc., Chem. Commun.*, 1994, 487.
2 S. Brooker and R. J. Kelly, *J. Chem. Soc., Dalton Trans.*, 1996, 2117.
3 S. Brooker, R. J. Kelly, B. Moubaraki and K. S. Murray, *Chem. Commun.*, 1996, 2579.
4 S. Brooker, R. J. Kelly and P. G. Plieger, *Chem. Commun.*, 1998, 1079.
5 S. Brooker, P. G. Plieger, B. Moubaraki and K. S. Murray, *Angew. Chem., Int. Ed.*, 1999, **38**, 408.
6 S. Brooker, S. J. Hay and P. G. Plieger, *Angew. Chem., Int. Ed.*, 2000, **39**, 1968.
7 S. Brooker, T. C. Davidson, S. J. Hay, R. J. Kelly, D. K. Kennepohl, P. G. Plieger, B. Moubaraki, K. S. Murray, E. Bill and E. Bothe, *Coord. Chem. Rev.*, 2001, **216–217**, 3.
8 S. Brooker, J. D. Ewing and J. Nelson, *Inorg. Chim. Acta*, 2001, **317**, 53.
9 See, for example: Y. Zhang, L. K. Thompson, M. Bubenik and J. N. Bridson, *J. Chem. Soc., Chem. Commun.*, 1993, 1375; T. Otieno, S. J. Rettig, R. C. Thompson and J. Trotter, *Inorg. Chem.*, 1995, **34**, 1718.
10 O. Kahn and C. Martinez, *Science*, 1998, **279**, 44.
11 O. Kahn, *Chem. Br.*, 1999, **2**, 24.
12 H. Toftlund, in *Magnetism: A Supramolecular Function*, ed. O. Kahn, NATO ASI Ser., Ser. C, Kluwer Academic Press, The Netherlands,1996, vol. 484, p. 323.
13 See, for example: P. J. van Konigsbruggen, Y. Garcia, H. Kooijman, A. L. Spek, J. G. Haasnoot, O. Kahn, J. Linares, E. Codjovi and F. Varret, *J. Chem. Soc., Dalton Trans.*, 2001, 466; O. Roubeau, J. M. A. Gomez, E. Balskus, J. J. A. Kolnaar, J. G. Haasnoot and J. Reedijk, *New J. Chem.*, 2001, **25**, 144; P. Gutlich, Y. Garcia and H. A. Goodwin, *Chem. Soc. Rev.*, 2000, **29**, 419; P. A. Anderson, T. Astley, M. A. Hitchman, F. R. Keene, B. Moubaraki, K. S. Murray, B. W. Skelton, E. R. T. Tiekink, H. Toftlund and A. H. White, *J. Chem. Soc., Dalton Trans.*, 2000, 3505; E. Breuning, M. Ruben, J.-M. Lehn, F. Renz, Y. Garcia, V. Ksenofontov, P. Gutlich, E. Wegelius and K. Rissanen, *Angew. Chem., Int. Ed.*, 2000, **39**, 2504; D. L. Reger, C. A. Little, A. L. Rheingold, M. Lam, T. Concolino, A. Mohan and G. J. Long, *Inorg. Chem.*, 2000, **39**, 4674 and ref. 37.
14 See, for example: A. B. Gaspar, M. C. Muñoz, V. Niel and J. A. Real, *Inorg. Chem.*, 2001, **40**, 9; R. Clerac, F. A. Cotton, K. R. Dunbar, T. B. Lu, C. A. Murillo and X. P. Wang, *J. Am. Chem. Soc.*, 2000, **122**, 2272; R. Sieber, S. Decurtins, H. Stoeckli-Evans, C. Wilson, D. Yufit, J. A. K. Howard, S. C. Capelli and A. Hauser, *Chem. Eur. J.*, 2000, **6**, 361; K. Heinze, G. Huttner, L. Zsolnai and P. Schober, *Inorg. Chem.*, 1997, **36**, 5457; P. Thuery and J. Zarembowitch, *Inorg. Chem.*, 1986, **25**, 200; J. Zarembowitch and O. Kahn, *Inorg. Chem.*, 1984, **23**, 589 and ref. 35.
15 E. Yeager, *Electrochim. Acta*, 1984, **29**, 1527.
16 J. E. Andrew, P. W. Ball and A. B. Blake, *Chem. Commun.*, 1969, 143.
17 P. W. Ball and A. B. Blake, *J. Chem. Soc., Dalton Trans.*, 1974, 852.
18 T. Wen, L. K. Thompson, F. L. Lee and E. J. Gabe, *Inorg. Chem.*, 1988, **27**, 4190.
19 A. Escuer, R. Vicente, B. Mernari, A. E. Gueddi and M. Pierrot, *Inorg. Chem.*, 1997, **36**, 2511.
20 J. A. Real, in *Transition Metals in Supramolecular Chemistry*, ed. J.-P. Sauvage, J. Wiley, Chichester, 1999, p. 53.
21 K. Buijs, *J. Chem. Phys.*, 1962, **36**, 861.
22 K. Nakamoto, *Infrared and Raman Spectra of Inorganic and Coordination Compounds, Part B*, John Wiley and Sons Inc., New York, 1997.
23 C. J. Harding, F. E. Mabbs, E. J. L. MacInnes, V. McKee and J. Nelson, *J. Chem. Soc., Dalton Trans.*, 1996, 3227.
24 W. J. Geary, *Coord. Chem. Rev.*, 1971, **7**, 81.
25 A. B. P. Lever, *Inorganic Electronic Spectroscopy*, Elsevier Science, Amsterdam, 1984.
26 C. Daul, C. W. Schlapfer and A. von Zelewsky, *Structure Bond.*, 1979, **36**, 129.
27 P. L. Orioli, *Coord. Chem. Rev.*, 1971, **6**, 285.
28 A. Bencini and D. Gatteschi, *EPR of Exchange Coupled Systems*, Springer-Verlag, Berlin/Heidelberg, 1990.
29 J. Faus, M. Julve, F. Lloret and M. C. Munoz, *Inorg. Chem.*, 1993, **32**, 2013.
30 P. Guionneau, J.-F. Letard, D. S. Yufit, D. Chasseau, G. Bravic, A. E. Goeta, J. A. K. Howard and O. Kahn, *J. Mater. Chem.*, 1999, **9**, 985.
31 O. Kahn, *Molecular Magnetism*, VCH Publishers Inc,New York, 1993.
32 G. De Munno, M. Julve, F. Lloret, J. Faus and A. Caneschi, *J. Chem. Soc., Dalton Trans.*, 1994, 1175.
33 J. Glerup, P. A. Goodson, D. J. Hodgson and K. Michelsen, *Inorg. Chem.*, 1995, **34**, 6255.
34 B. Bleaney and K. D. Bowers, *Proc. R. Soc. London, Ser. A*, 1952, **214**, 451.
35 B. J. Kennedy, G. D. Fallon, B. M. K. C. Gatehouse and K. S. Murray, *Inorg. Chem.*, 1984, **23**, 580.
36 F. S. Keij, R. A. G. de Graaff, J. G. Haasnoot and J. Reedijk, *J. Chem. Soc., Dalton Trans.*, 1984, 2093.
37 J.-F. Letard, J. A. Real, N. Moliner, A. B. Gaspar, L. Capes, O. Cador and O. Kahn, *J. Am. Chem. Soc.*, 1999, **121**, 10630.
38 G. M. Sheldrick, *Acta Crystallogr., Sect. A*, 1990, **46**, 467.
39 G. M. Sheldrick, *Methods Enzymol.*, 1997, **276**, 628.
40 G. M. Sheldrick and T. R. Schneider, *Methods Enzymol.*, 1997, **277**, 319.